J. Fluid Mech. (1993), *vol.* 249, *pp.* 597–618

Weakly nonlinear stability of viscous vortices in three-dimensional boundary layers

By ANDREW P. BASSOM[1] AND S. R. OTTO[2]

[1] Department of Mathematics, University of Exeter, North Park Road, Exeter, Devon EX4 4QE, UK

[2] ICASE, Mailstop 132c, NASA Langley Research Center, Hampton, VA 23665-5225, USA

(Received 6 April 1992 and in revised form 15 September 1992)

Recently it has been demonstrated that three-dimensionality can play an important role in dictating the stability of any Görtler vortices which a particular boundary layer may support. According to a linearized theory, vortices within a high Görtler number flow can take one of two possible forms within a two-dimensional flow supplemented by a small crossflow of size $O(Re^{-\frac{1}{3}}G^{\frac{2}{5}})$, where Re is the Reynolds number of the flow and G the Görtler number. Bassom & Hall (1991) showed that these forms are characterized by $O(1)$-wavenumber inviscid disturbances and larger $O(G^{\frac{1}{5}})$-wavenumber modes which are trapped within a thin layer adjacent to the bounding surface. Here we concentrate on the latter, essentially viscous, vortices. These modes are unstable in the absence of crossflow but the imposition of small crossflow has a stabilizing effect. Bassom & Hall (1991) demonstrated the existence of neutrally stable vortices for certain crossflow/wavenumber combinations and here we describe the weakly nonlinear stability properties of these disturbances. It is shown conclusively that the effect of crossflow is to stabilize the nonlinear modes and the calculations herein allow stable finite-amplitude vortices to be found. Predictions are made concerning the likelihood of observing some of these viscous modes within a practical setting and asymptotic work permits discussion of the stability properties of modes with wavenumbers that are small relative to the implied $O(G^{\frac{1}{5}})$ scaling.

1. Introduction

Over the past 50 years there has been interest in the stability properties of Görtler vortices within boundary-layer flows. Early studies ignored non-parallel effects present due to boundary-layer growth; the importance of this phenomenon was first explained by the results of Hall (1982*a*, *b*, 1983). In that series of papers Hall showed, using both asymptotic and numerical methods, that for vortices of order-one wavenumber there is no unique neutral linear stability curve and the stability characteristics of such wavenumber modes are entirely dependent upon the initial form and location of the disturbance. However, for small-wavelength vortices a unique neutral curve does exist and on this curve the vortex wavenumber k is $O(G^{\frac{1}{4}})$ where G is the (large) Görtler number. For an extensive review of the development of stability theory pertinent to Görtler vortices the reader is referred to Hall (1990).

The most unstable Görtler mode was obtained by Denier, Hall & Seddougui (1991) and Timoshin (1990). These authors showed that according to linearized theory the vortices with largest growth rates have wavenumbers within the $O(G^{\frac{1}{5}})$ regime and the corresponding amplification rates are then $O(G^{\frac{3}{5}})$. The exact stability properties of $O(G^{\frac{1}{5}})$-wavenumber vortices are derived by solving a sixth-order ordinary differential

system and the solution of this system reveals that the unique most unstable mode has wavenumber $k = 0.476G^{\frac{1}{5}}$ and growth rate $0.312G^{\frac{3}{5}}$.

Much of the work to date concerned with the stability of Görtler vortices has concentrated on two-dimensional boundary-layer flows, but in many practical situations in which Görtler vortices are known to arise the basic boundary layer is three-dimensional. For example, in the case of a boundary-layer flow over an obstacle or the flow over a turbine blade the three-dimensionality of the basic flow is potentially crucial. In particular, the development of laminar-flow airfoils has given rise to designs that have two areas of concave curvature on the lower side of the airfoil: in this case when the wing is swept the boundary-layer flow is fully three-dimensional.

The first attempt to describe the effect of three-dimensionality was given by Hall (1985) who examined the Görtler mechanism in flow over an infinitely long swept cylinder. It was shown that it is the relative size of the crossflow and chordwise flow over the cylinder that is critical in determining the vortex structure. The neutral Görtler number for the vortices was predicted by a large-wavenumber asymptotic analysis, the results of which suggested that for $O(1)$ values of the ratio of the crossflow and chordwise velocity fields the Görtler mechanism is probably unimportant compared with Tollmien–Schlichting and crossflow-type instabilities. Indeed, there is some limited experimental evidence that supports this conclusion. Work by Baskaran & Bradshaw (1988) has shown, at least for turbulent boundary layers, that increasing the crossflow velocity component tends to destroy the Görtler mechanism.

Bassom & Hall (1991) (hereafter referred to as BH) extended the work of Denier *et al.* (1991) to consider the effect of introducing crossflow into the boundary-layer flow. Like Denier *et al.*, BH conducted a spatial stability analysis of the vortex modes and they demonstrated that for $O(1)$-wavenumber modes at large Görtler numbers the crossflow first has significant effect on the two-dimensional results once it becomes $O(Re^{-\frac{1}{2}}G^{\frac{1}{2}})$, where Re is the Reynolds number of the flow. As the crossflow increases, the stationary vortex structure takes on an identity which is essentially that of a crossflow instability; a mechanism first investigated by Gregory, Stuart & Walker (1955). BH also obtained a description of the influence of crossflow on the $O(G^{\frac{1}{5}})$-wavenumber (viscous) vortices of Denier *et al.* (1991). It was shown that when the ratio of crossflow to chordwise flow becomes $O(Re^{-\frac{1}{2}}G^{\frac{3}{5}})$ the results of Denier *et al.* need to be modified: significantly it was demonstrated that the introduction of crossflow into the problem has a stabilizing effect, at least according to linear stability theory. Whereas in Denier *et al.* it was proved that stationary vortices are necessarily unstable at $O(G^{\frac{1}{5}})$ wavenumbers, this is no longer true once crossflow terms are introduced. In addition, for certain crossflow values there exist neutrally stable vortex modes whilst at large enough values of the crossflow no vortex structures induced by centrifugal effects can exist.

The aim of the present paper is to extend BH by studying the weakly nonlinear stability characteristics of the $O(G^{\frac{1}{5}})$-wavenumber modes. Denier & Hall (1993) have made a numerical study of the fully nonlinear evolution of these high-wavenumber structures within a two-dimensional boundary layer. They have shown that the nonlinear equations governing the Görtler vortex over an $O(G^{-\frac{2}{5}})$ streamwise lengthscale are fully non-parallel in nature. By implementing the computational scheme developed by Hall (1988), Denier & Hall illustrated that given a suitable initial perturbation then eventually the energy of the higher harmonics grows until a singularity is encountered at some downstream position. It is concluded that it is this singularity that is ultimately the cause of vortices which are originally close to the wall moving into the main part of the boundary layer.

Although extensive calculations will eventually be desirable in order to assess the fully nonlinear stability properties of Görtler vortices within three-dimensional boundary layers, here we shall consider a more analytical weakly nonlinear approach. This case is not without interest for it is likely to be of importance in the stability of several flows occurring in practice. In Denier *et al.* (1991) studies were made of the receptivity of boundary layers to Görtler vortices. Typically, small disturbances in the boundary layer or small surface imperfections make the flow susceptible to vortices and since these disturbances or imperfections are usually of small dimension it is the high-wavenumber vortices that are often excited. This then suggests that modes of $O(G^{\frac{1}{5}})$ wavenumber (i.e. within the wavenumber regime containing the most unstable linear mode) will perhaps be favoured in preference to the larger scale $O(1)$-wavenumber inviscid modes. We have already mentioned that in the absence of crossflow all steady Görtler modes of $O(G^{\frac{1}{5}})$ wavenumber are unstable but the addition of a small crossflow stabilizes the situation and, in particular, certain crossflow/wavenumber combinations lead to linearly neutrally stable modes. In consequence, a small surface imperfection may well trigger modes which, although linearly unstable, are only marginally so and then a weakly nonlinear analysis is of relevance in determining whether these modes grow without bound or whether nonlinear effects exert a stabilizing influence and lead to finite-amplitude stable states as the vortices develop downstream.

The remainder of the paper is divided as follows. In the coming section the problem is formulated and the weakly nonlinear equations are obtained. The numerical methods implemented to solve these equations are described in §3 and the nonlinear properties of the modes examined in §4. Section 5 addresses the low-wavenumber limit of the amplitude equation, and we close with some discussion.

2. Derivation of the weakly nonlinear equations

Our aim is to derive the equations which determine weakly nonlinear high-wavenumber viscous vortex modes in a slightly three-dimensional boundary layer. Following Hall (1985) we consider the boundary layer flowing over the cylinder $y = 0$, $-\infty < x < \infty$, where the z-axis is a generator of the cylinder, y is the distance normal to the surface and the x-coordinate measures distance along the curved surface. Suppose that this surface has variable curvature

$$(1/b)\,\chi(x/l), \tag{2.1a}$$

where b is a typical radius of curvature of the surface and l is a characteristic lengthscale in the streamwise direction. The Reynolds number Re, the curvature parameter δ and the Görtler number G are defined by

$$Re = U_0 l/\nu, \quad \delta = l/b, \quad G = 2Re^{\frac{1}{2}}\delta, \tag{2.1b–d}$$

where U_0 is a typical flow speed in the x-direction and ν is the kinematic viscosity of the fluid. Our interest is in the limit of $Re \gg 1$ and $\delta \ll 1$ such that in the limit $\delta \to 0$ G is held fixed at an $O(1)$ value. The basic flow is taken to be of the form

$$\boldsymbol{u} = U_0(\bar{u}(X, Y), Re^{-\frac{1}{2}}\bar{v}(X, Y), Re^{-\frac{1}{2}}\lambda^*\bar{w}(X, Y))(1 + O(Re^{-\frac{1}{2}})), \tag{2.2}$$

where $X = x/l$ and $Y = yRe^{\frac{1}{2}}/l$, and the crossflow parameter λ^* is of order one.

It is convenient to define the scaled spanwise coordinate $Z = Re^{\frac{1}{2}}z/l$ and let t be the temporal variable scaled on l/U_0. The basic velocity profile is perturbed by

$$(U(t, X, Y, Z), Re^{-\frac{1}{2}}V(t, X, Y, Z), Re^{-\frac{1}{2}}W(t, X, Y, Z)), \tag{2.3a}$$

the pressure field is given by

$$p = \bar{p}(X) + Re^{-1}P(t, X, Y, Z), \tag{2.3b}$$

and on substituting (2.3) into the continuity and Navier–Stokes equations we obtain

$$U_X + V_Y + W_Z = 0, \tag{2.4a}$$

$$-U_t + U_{YY} + U_{ZZ} - \bar{u}_Y V - \bar{u}U_X - \bar{u}_X U - \bar{v}U_Y - \lambda^* \bar{w}U_Z = UU_X + VU_Y + WU_Z, \tag{2.4b}$$

$$-V_t + V_{YY} + V_{ZZ} - G\chi\bar{u}U - P_Y - \bar{u}V_X - \bar{v}_X U - \bar{v}V_Y - \bar{v}_Y V - \lambda^* \bar{w}V_Z = UV_X + VV_Y + WV_Z + G\chi U^2/2, \tag{2.4c}$$

$$-W_t + W_{YY} + W_{ZZ} - P_Z - \bar{u}W_X - \lambda^* \bar{w}_X U - \bar{v}W_Y - \lambda^* V\bar{w}_Y - \lambda^* \bar{w}W_Z = UW_X + VW_Y + WW_Z, \tag{2.4d}$$

where terms of relative order $Re^{-\frac{1}{2}}$ have been neglected.

We now follow the scalings first derived by Denier *et al.* (1991) in which it was shown that the $O(G^{\frac{1}{5}})$-wavenumber vortices are confined to a layer of thickness $O(G^{-\frac{1}{5}})$ adjacent to the cylinder. These modes have a spatial growth rate $O(G^{\frac{3}{5}})$, and it was proved in **BH** that the three-dimensionality of the basic flow is first significant for these viscous vortices once the scaled crossflow λ^* is $O(G^{\frac{2}{5}})$. Therefore it is convenient to define the $O(1)$ crossflow parameter $\hat{\lambda}$ by

$$\lambda^* = G^{\frac{2}{5}}\hat{\lambda}. \tag{2.5a}$$

If the spanwise wavenumber of the fundamental vortex is taken to be a (which, recall, is $O(G^{\frac{1}{5}})$) then the scaled wavenumber k_0 is defined according to

$$a = k_0 G^{\frac{1}{5}}, \tag{2.5b}$$

and the disturbance is confined to the region where the coordinate ψ given by

$$\psi = k_0 G^{\frac{1}{5}} Y, \tag{2.5c}$$

is of order one. In **BH** linearized disturbances were sought proportional to

$$E_1 \equiv \exp\left[ik_0 G^{\frac{1}{5}}Z + G^{\frac{4}{5}}\int^X (\beta_0 + G^{-\frac{1}{5}}\beta_1(X) + \ldots)\,\mathrm{d}X - iG^{\frac{2}{5}}\int^t (\Omega_0(t) + G^{-\frac{1}{5}}\Omega_1(t) + \ldots)\,\mathrm{d}t\right], \tag{2.6}$$

where this definition reflects the fact that the vortex has spanwise wavenumber $O(G^{\frac{1}{5}})$ and the disturbance has an $O(G^{\frac{3}{5}})$ growth rate (since it transpires that β_0 is purely imaginary). Furthermore, for small Y the basic flow quantities $\bar{u}$ and $\bar{w}$ are assumed to take the forms

$$\bar{u} = \mu_{11}(X)\,Y + [\mu_{12}(X)/2!]\,Y^2 + [\mu_{13}(X)/3!]\,Y^3 + \ldots, \tag{2.7a}$$

$$\bar{w} = \mu_{21}(X)\,Y + [\mu_{22}(X)/2!]\,Y^2 + [\mu_{23}(X)/3!]\,Y^3 + \ldots, \tag{2.7b}$$

and $\bar{v} = O(Y^2)$. To extend the work of **BH** to weakly nonlinear modes necessitates considering expressions of the form

$$U = G^{-\frac{1}{5}}[h(U_{011}E_1 + \text{c.c.}) + h^2(U_{022}E_1^2 + \text{c.c.} + U_{020}) + h^3(U_{031}E_1 + \text{c.c.}) + \ldots] + G^{-\frac{2}{5}}[h(U_{111}E_1 + \text{c.c.}) + h^2(U_{122}E_1^2 + \text{c.c.} + U_{120}) + h^3(U_{131}E_1 + \text{c.c.}) + \ldots], \tag{2.8}$$

with similar expressions for $G^{-\frac{2}{5}}V$, $G^{-\frac{3}{5}}W$ and $G^{-\frac{3}{5}}P$ (c.c. denotes complex conjugate). Here all the unknown coefficients $U_{011}, U_{022}, \ldots$ are functions of the scaled coordinate ψ alone and h is taken to be a parameter, $0 < h \ll 1$, such that expansions in h are taken

after expansion in the small parameter $G^{-\frac{1}{5}}$. Furthermore, the wavenumber β_1 and frequency Ω_0 need to be expanded in terms of h as in the usual Stuart–Watson (1960) approach and details of this will be given presently.

Derivation of the required evolution equation is a relatively straightforward though slightly lengthy process. The methodology is similar to that employed by BH and thus we shall indicate how this is tackled for the leading-order disturbance quantities U_{011}, V_{011}, W_{011} and P_{011}. Given this information, the ensuing calculations follow almost identical lines so that only the final results need be stated.

The vortex equations are deduced by substituting (2.5)–(2.8) in (2.4) and comparing coefficients of like powers of G and h. The continuity equation (2.4a) yields

$$\beta_0 U_{011} + \mathrm{i}k_0 W_{011} = 0, \tag{2.9a}$$

$$\beta_1 U_{011} + \beta_0 U_{111} + \mathrm{i}k_0 W_{111} + k_0(\mathrm{d}V_{011}/\mathrm{d}\psi) = 0. \tag{2.9b}$$

The streamwise and spanwise momentum equations (2.4b, d) then give

$$\beta_0 U_{020} + \mathrm{i}k_0 W_{020} = -[(\beta_0 \mu_{11}/k_0) + \mathrm{i}\hat{\lambda}\mu_{21}]\psi, \tag{2.10}$$

but the constraint that the disturbance be confined to the thin wall layer requires that U_{020}, W_{020} remain bounded as $\psi \to \infty$, which in turn forces the relationship

$$(\beta_0 \mu_{11}/k_0) + \mathrm{i}\hat{\lambda}\mu_{21} = 0. \tag{2.11a}$$

This confirms the assertion that β_0 is purely imaginary and then (2.10) becomes

$$\beta_0 U_{020} + \mathrm{i}k_0 W_{020} = 0. \tag{2.11b}$$

Next-order terms in the streamwise momentum equation lead to the equation

$$\left[\frac{\mathrm{d}^2}{\mathrm{d}\psi^2} - 1 + \frac{\mathrm{i}\Omega_0}{k_0^2} - \frac{\beta_1 \mu_{11}}{k_0^3}\psi - \frac{\mathrm{i}\hat{\lambda}(\mu_{11}\mu_{22} - \mu_{12}\mu_{21})}{2k_0^3 \mu_{11}}\psi^2\right] U_{011} - \frac{\mu_{11}}{k_0^2} V_{011} = 0. \tag{2.12}$$

The second equation for the leading-order vortex components is obtained by following the scheme outlined in BH. Order-$G^{\frac{4}{5}}$ terms in the momentum equation (2.4c) enable a relation for the leading-order pressure gradient to be derived in the form

$$\frac{\mathrm{d}P_{011}}{\mathrm{d}\psi} = k_0\left[\frac{\mathrm{d}^2}{\mathrm{d}\psi^2} - 1 + \frac{\mathrm{i}\Omega_0}{k_0^2} - \frac{\beta_1 \mu_{11}}{k_0^3}\psi - \frac{\mathrm{i}\hat{\lambda}(\mu_{11}\mu_{22} - \mu_{12}\mu_{21})}{2k_0^3 \mu_{11}}\psi^2\right] V_{011} - \frac{\mu_{11}\chi_0 \psi}{k_0^2} U_{011}, \tag{2.13}$$

where here we have denoted by χ_0 the value of the curvature parameter χ taken at the downstream location at which the vortex motions are being studied. Additionally, $O(G^{\frac{1}{5}})$ and $O(G^{\frac{4}{5}})$ terms in the streamwise momentum equation (2.4b) and the spanwise momentum equation (2.4d) respectively show that

$$\left[\frac{\mathrm{d}^2}{\mathrm{d}\psi^2} - 1 + \frac{\mathrm{i}\Omega_0}{k_0^2} - \frac{\beta_1 \mu_{11}\psi}{k_0^3} - \frac{\mathrm{i}\hat{\lambda}(\mu_{11}\mu_{22} - \mu_{21}\mu_{12})\psi^2}{2k_0^3 \mu_{11}}\right] U_{111} = \frac{\mu_{11} V_{111}}{k_0^2}, \tag{2.14a}$$

$$\left[\frac{\mathrm{d}^2}{\mathrm{d}\psi^2} - 1 + \frac{\mathrm{i}\Omega_0}{k_0^2} - \frac{\beta_1 \mu_{11}\psi}{k_0^3} - \frac{\mathrm{i}\hat{\lambda}(\mu_{11}\mu_{22} - \mu_{21}\mu_{12})\psi^2}{2k_0^3 \mu_{11}}\right] W_{111} = \frac{\hat{\lambda}\mu_{21} V_{111}}{k_0^2} + \frac{\mathrm{i}}{k_0} P_{011}. \tag{2.14b}$$

Adding β_0 multiples of (2.14a), $\mathrm{i}k_0$ multiples of (2.14b) and β_1 multiples of (2.12), differentiating the resulting equation with respect to ψ and substituting for $\mathrm{d}P_{011}/\mathrm{d}\psi$ according to (2.13) leads to the required second equation relating the leading-order vortex quantities.

As in BH it is convenient to invoke the scalings

$$k_0 = (\chi_0 \mu_{11}^2)^{\frac{1}{5}} k, \quad \beta_1 = \mathrm{i}\chi_0^{\frac{3}{5}} \mu_{11}^{\frac{1}{5}} \beta, \quad U_{0jk} = \chi_0^{-\frac{1}{5}} \mu_{11}^{\frac{3}{5}} U_{jk}, \tag{2.15a–c}$$

$$V_{0jk} = \chi_0^{\frac{1}{5}} \mu_{11}^{\frac{2}{5}} V_{jk}, \quad \Omega_0 = -\chi_0^{\frac{2}{5}} \mu_{11}^{\frac{4}{5}} \Omega, \quad \lambda = \tfrac{1}{2}\hat{\lambda}(\mu_{11}\mu_{22} - \mu_{21}\mu_{12}) \mu_{11}^{-\frac{1}{5}} \chi_0^{-\frac{3}{5}}, \tag{2.15d–f}$$

where the notation U_{0jk}, V_{0jk} in (2.15*c*, *d*) denotes that we apply this scaling to all the components of these general types in (2.8). These reductions lead to the equations as presented in BH for the leading-order vortex terms U_{11} and V_{11}, viz.

$$\left(\frac{\mathrm{d}^2}{\mathrm{d}\psi^2} - 1 - \frac{\mathrm{i}\Omega}{k^2} - \frac{\mathrm{i}\beta\psi}{k^3} - \frac{\mathrm{i}\lambda\psi^2}{k^3}\right) U_{11} - \frac{V_{11}}{k^2} = 0, \tag{2.16a}$$

$$\left(\frac{\mathrm{d}^2}{\mathrm{d}\psi^2} - 1 - \frac{\mathrm{i}\Omega}{k^2} - \frac{\mathrm{i}\beta\psi}{k^3} - \frac{\mathrm{i}\lambda\psi^2}{k^3}\right)\left(\frac{\mathrm{d}^2}{\mathrm{d}\psi^2} - 1\right) V_{11} + \frac{2\mathrm{i}\lambda}{k^3} V_{11} + \frac{\psi}{k^3} U_{11} = 0. \tag{2.16b}$$

Notice that the scaling (2.15*b*) ensures that neutrally stable modes correspond to the case when the scaled parameter β is purely real valued.

To complete our derivation of the evolution equation for the weakly nonlinear mode then, in keeping with the usual approach, we need to perturb the streamwise variation parameter β and scaled frequency Ω from their neutral values, say β_{n} and Ω_{n} respectively, by $O(h^2)$ quantities. Therefore we write

$$\beta = \beta_{\mathrm{n}} + h^2\hat{\beta} + \ldots, \quad \Omega = \Omega_{\mathrm{n}} + h^2\hat{\Omega} + \ldots, \tag{2.17a, b}$$

where terms of $o(h^2)$ need not be specified as they are too small to affect our results. It is convenient to define the operator L_N by

$$\mathrm{L}_N \equiv \frac{\mathrm{d}^2}{\mathrm{d}\psi^2} - N^2 - \frac{\mathrm{i}\Omega_{\mathrm{n}} N}{k^2} - \frac{\mathrm{i}\beta_{\mathrm{n}} N\psi}{k^3} - \frac{\mathrm{i}\lambda N\psi^2}{k^3} \tag{2.18}$$

and with this definition the leading-order system (2.16) may be written as

$$\mathrm{L}_1(U_{11}) - \frac{V_{11}}{k^2} = 0, \quad \mathrm{L}_1\left(\frac{\mathrm{d}^2}{\mathrm{d}\psi^2} - 1\right) V_{11} + \frac{2\mathrm{i}\lambda}{k^3} V_{11} + \frac{\psi}{k^3} U_{11} = 0, \tag{2.19a, b}$$

which needs to be solved subject to the conditions

$$U_{11}, \quad V_{11}, \quad \mathrm{d}V_{11}/\mathrm{d}\psi \to 0 \quad \text{as} \quad \psi \to 0, \infty, \tag{2.19c}$$

in order to ensure zero disturbance quantities on the surface $Y = 0$ and that the vortex decays as $Y \to \infty$.

To continue the process of obtaining governing equations for the remaining $O(G^{-\frac{1}{5}})$ terms within the original expansions (2.8) is merely a matter of repeating the steps outlined in (2.9)–(2.14). The only new feature is that nonlinear terms begin to enter the analysis, but this causes no formal difficulties. Since this process has been illustrated above we merely state the solutions at each order of the analysis.

Recalling the scalings (2.15) it is found that the harmonic terms V_{22} and U_{22} satisfy

$$\mathrm{L}_2(U_{22}) - \frac{V_{22}}{k^2} = \frac{1}{k}\left(\frac{\mathrm{d}U_{11}}{\mathrm{d}\psi} V_{11} - U_{11}\frac{\mathrm{d}V_{11}}{\mathrm{d}\psi}\right), \tag{2.20a}$$

$$\mathrm{L}_2\left(\frac{\mathrm{d}^2}{\mathrm{d}\psi^2} - 4\right) V_{22} + \frac{4\mathrm{i}\lambda}{k^3} V_{22} + \frac{4\psi}{k^3} U_{22} = \frac{2}{k}\left(V_{11}\frac{\mathrm{d}^3 V_{11}}{\mathrm{d}\psi^3} - 2\frac{\mathrm{d}V_{11}}{\mathrm{d}\psi}\frac{\mathrm{d}^2 V_{11}}{\mathrm{d}\psi^2}\right) - \frac{2}{k^2} U_{11}^2, \tag{2.20b}$$

subject to the boundary conditions that

$$U_{22}, \quad V_{22}, \quad \mathrm{d}V_{22}/\mathrm{d}\psi \to 0 \quad \text{as} \quad \psi \to 0, \infty. \tag{2.20c}$$

Furthermore, the mean flow correction terms U_{20} and V_{20} are given by

$$U_{20} = \int_0^{\psi} \{(U_{11} V_{11}^* + \text{c.c.})/k\} \, \mathrm{d}\psi, \quad V_{20} = 0, \tag{2.21}$$

where here, and henceforth, an asterisk used on a quantity denotes its complex conjugate.

In order to derive the evolution equation for the vortex it is necessary to proceed to $O(h^3)$ terms in expansions (2.8). The $O(h^3)$ terms of importance are those proportional to E_1 and these quantities, U_{031} and V_{031}, or in their scaled forms, U_{31} and V_{31}, satisfy

$$\mathrm{L}_1(U_{31}) - \frac{V_{31}}{k^2} = \left(\frac{\mathrm{i}\hat{\Omega}}{k^2} + \frac{\mathrm{i}\hat{\beta}\psi}{k^3}\right) U_{11} + \frac{1}{k}\left(\frac{\mathrm{d}U_{11}^*}{\mathrm{d}\psi} V_{22} + \frac{\mathrm{d}U_{20}}{\mathrm{d}\psi} V_{11} + \frac{\mathrm{d}U_{22}}{\mathrm{d}\psi} V_{11}^* + \frac{U_{11}^*}{2}\frac{\mathrm{d}V_{22}}{\mathrm{d}\psi} + 2U_{22}\frac{\mathrm{d}V_{11}^*}{\mathrm{d}\psi}\right) + \frac{U_{11}\Phi_0}{k^2}, \tag{2.22a}$$

$$\mathrm{L}_1\left(\frac{\mathrm{d}^2}{\mathrm{d}\psi^2} - 1\right) V_{31} + \frac{2\mathrm{i}\lambda}{k^3} V_{31} + \frac{\psi U_{31}}{k^3} = \left(\frac{\mathrm{i}\hat{\Omega}}{k^2} + \frac{\mathrm{i}\hat{\beta}\psi}{k^3}\right)\left(\frac{\mathrm{d}^2}{\mathrm{d}\psi^2} - 1\right) V_{11} + \frac{1}{k^2}\left(\Phi_0\left(\frac{\mathrm{d}^2}{\mathrm{d}\psi^2} - 1\right) V_{11} - V_{11}\frac{\mathrm{d}^2\Phi_0}{\mathrm{d}\psi^2} - U_{11}^* U_{22} - U_{20} U_{11}\right) - \frac{1}{k}\left(3V_{22}\frac{\mathrm{d}V_{11}^*}{\mathrm{d}\psi} + \tfrac{3}{2}V_{11}^*\frac{\mathrm{d}V_{22}}{\mathrm{d}\psi} - \frac{\mathrm{d}V_{11}^*}{\mathrm{d}\psi}\frac{\mathrm{d}^2V_{22}}{\mathrm{d}\psi^2} + \frac{1}{2}\frac{\mathrm{d}V_{22}}{\mathrm{d}\psi}\frac{\mathrm{d}^2V_{11}^*}{\mathrm{d}\psi^2} + V_{22}\frac{\mathrm{d}^3V_{11}^*}{\mathrm{d}\psi^3} - \frac{V_{11}^*}{2}\frac{\mathrm{d}^3V_{22}}{\mathrm{d}\psi^3}\right), \tag{2.22b}$$

where

$$\Phi_0 = \int_0^{\psi}\left(V_{11}\frac{\mathrm{d}V_{11}^*}{\mathrm{d}\psi} - V_{11}^*\frac{\mathrm{d}V_{11}}{\mathrm{d}\psi}\right)\mathrm{d}\psi, \tag{2.22c}$$

and (2.22*a*, *b*) are subject to the boundary conditions

$$U_{31}, \quad V_{31}, \quad \mathrm{d}V_{31}/\mathrm{d}\psi \to 0 \quad \text{as} \quad \psi \to 0, \infty. \tag{2.22d}$$

The homogeneous forms of (2.22) are merely (2.19) and so, as is the normal method within a weakly nonlinear analysis, equations (2.22) only have a suitable solution if a certain compatibility condition is satisfied. This condition leads to the specification of the correction terms $\hat{\beta}$ and $\hat{\Omega}$ within the streamwise dependence and frequency expansions detailed by (2.17). To derive the compatibility requirement it is necessary to first consider the system adjoint to the homogeneous equations (2.19). This adjoint system consists of the functions $\hat{F}(\psi)$ and $\hat{G}(\psi)$ which are the solutions of the coupled equations

$$\mathrm{L}_1(\hat{F}) + \frac{\psi}{k^3}\hat{G} = 0, \tag{2.23a}$$

$$\frac{\mathrm{d}^4\hat{G}}{\mathrm{d}\psi^4} - \left(2 + \frac{\mathrm{i}\Omega_{\mathrm{n}}}{k^2} + \frac{\mathrm{i}\beta_{\mathrm{n}}\psi}{k^3} + \frac{\mathrm{i}\lambda\psi^2}{k^3}\right)\frac{\mathrm{d}^2\hat{G}}{\mathrm{d}\psi^2} - \left(\frac{2\mathrm{i}\beta_{\mathrm{n}}}{k^3} + \frac{4\mathrm{i}\lambda\psi}{k^3}\right)\frac{\mathrm{d}\hat{G}}{\mathrm{d}\psi} + \left(\frac{\mathrm{i}\lambda\psi^2}{k^3} + \frac{\mathrm{i}\beta_{\mathrm{n}}\psi}{k^3} + \frac{\mathrm{i}\Omega_{\mathrm{n}}}{k^2} + 1\right)\hat{G} - \frac{\hat{F}}{k^2} = 0, \tag{2.23b}$$

with the associated conditions that $\hat{F}$, $\hat{G}$ and $\mathrm{d}\hat{G}/\mathrm{d}\psi \to 0$ as $\psi \to 0, \infty$. Before proceeding further we should comment upon our definition of the amplitude of the vortex mode. Clearly the system (2.19) which determines the functions U_{11} and V_{11} is linear and so we have an arbitrary factor at our disposal. Therefore, for definiteness, we shall call $\{\mathrm{d}U_{11}/\mathrm{d}\psi\}_{\psi=0}$ the scaled amplitude A of the vortex. Of course there are many other definitions we could use for this amplitude but this one is as good as any other. To obtain the equation for the vortex amplitude A it is seen (by multiplying (2.22a) by $\hat{F}$, (2.22b) by $\hat{G}$, adding and integrating with respect to ψ) that for a solution of (2.22) to exist it is necessary that

$$z_1 \hat{\beta} A + z_2 \hat{\Omega} A = -I_* A|A|^2,$$

where

$$z_1 \equiv \frac{\mathrm{i}}{k^3}\int_0^\infty \left(\hat{F}\psi U_{11} + \hat{G}\psi\left(\frac{\mathrm{d}^2}{\mathrm{d}\psi^2} - 1\right)V_{11}\right)\mathrm{d}\psi, \tag{2.24a}$$

$$z_2 \equiv \frac{\mathrm{i}}{k^2}\int_0^\infty \left(\hat{F}U_{11} + \hat{G}\left(\frac{\mathrm{d}^2}{\mathrm{d}\psi^2} - 1\right)V_{11}\right)\mathrm{d}\psi, \tag{2.24b}$$

and $I_* \equiv \int_0^\infty H\,\mathrm{d}\psi$, where

$$\begin{aligned} H = {} & \frac{\hat{F}}{k}\left(\frac{\mathrm{d}U_{11}^*}{\mathrm{d}\psi}V_{22} + \frac{\mathrm{d}U_{20}}{\mathrm{d}\psi}V_{11} + \frac{\mathrm{d}U_{22}}{\mathrm{d}\psi}V_{11}^* + \frac{U_{11}^*}{2}\frac{\mathrm{d}V_{22}}{\mathrm{d}\psi} + 2U_{22}\frac{\mathrm{d}V_{11}^*}{\mathrm{d}\psi}\right) + \frac{\hat{F}U_{11}\Phi_0}{k^2} \\ & + \frac{\hat{G}}{k^2}\left(\Phi_0\left(\frac{\mathrm{d}^2}{\mathrm{d}\psi^2} - 1\right)V_{11} - V_{11}\frac{\mathrm{d}^2\Phi_0}{\mathrm{d}\psi^2} - U_{11}^* U_{22} - U_{20}U_{11}\right) \\ & - \frac{\hat{G}}{k}\left(3V_{22}\frac{\mathrm{d}V_{11}^*}{\mathrm{d}\psi} + \tfrac{3}{2}V_{11}^*\frac{\mathrm{d}V_{22}}{\mathrm{d}\psi} - \frac{\mathrm{d}V_{11}^*}{\mathrm{d}\psi}\frac{\mathrm{d}^2V_{22}}{\mathrm{d}\psi^2} + \frac{1}{2}\frac{\mathrm{d}V_{22}}{\mathrm{d}\psi}\frac{\mathrm{d}^2V_{11}^*}{\mathrm{d}\psi^2} + V_{22}\frac{\mathrm{d}^3V_{11}^*}{\mathrm{d}\psi^3} - \frac{V_{11}^*}{2}\frac{\mathrm{d}^3V_{22}}{\mathrm{d}\psi^3}\right). \end{aligned} \tag{2.24c}$$

The above analysis may be easily generalized so that the vortex evolves on a slow lengthscale and thence the growth or decay of a near neutral disturbance may be monitored. Formally, if we consider the neighbourhood of the point $X = X_\mathrm{n}$ (the point at which an infinitesimal vortex is neutrally stable) and allow a constant-frequency disturbance to develop on a lengthscale $\tilde{X}$ where $\tilde{X} = G^{-\frac{3}{5}}h^{-2}(X - X_\mathrm{n})$ with $h \ll 1$, then the result of repeating the previous analysis for a disturbance of amplitude $A(\tilde{X})$ relative to the scalings implied in (2.8) is the evolution equation

$$\frac{\mathrm{d}A}{\mathrm{d}\tilde{X}} = \left(-\frac{\mathrm{i}z_2}{z_1}\right)\hat{\Omega}A - \left(\frac{\mathrm{i}I_*}{z_1}\right)A|A|^2. \tag{2.25a}$$

It is then simple to derive the equation for the vortex amplitude:

$$\frac{\mathrm{d}}{\mathrm{d}\tilde{X}}(|A|^2) = c_1\hat{\Omega}|A|^2 + c_2|A|^4, \tag{2.25b}$$

where

$$c_1 \equiv 2\,\mathrm{Re}(-\mathrm{i}z_2/z_1), \quad c_2 \equiv 2\,\mathrm{Re}(-\mathrm{i}I_*/z_1). \tag{2.25c, d}$$

In order to evaluate the coefficients in (2.25b) it is necessary to solve the systems (2.19), (2.20) and (2.23) so that the expressions for z_1, z_2 and I_* as defined in (2.24) may be found.

Finally, it is clear that if $(\Omega_\mathrm{n}, \beta_\mathrm{n}, \lambda)$ is an eigenset of (2.19) then so is $(-\Omega_\mathrm{n}^*, -\beta_\mathrm{n}^*, -\lambda)$ for real crossflows λ. Evidently, it is possible to restrict our attention to positive

crossflow parameters without any loss of generality, and this is done for the remainder of the paper.

3. Numerical methods and preliminary calculations

In the context of their work on the viscous vortices BH were solely concerned with the numerical solution of the linear system (2.19). Their computations were based on a technique originally proposed by Malik, Chuang & Hussaini (1982) in which the differential equations to be solved are reduced to a set of linear algebraic equations using either a finite difference discretization or a spectral representation and the eigenvalues found by solving the characteristic determinant of a generalized eigenvalue problem. The particular method described in Malik *et al.* uses a fourth-order-accurate Euler–Maclaurin scheme with nodal points distributed so as to resolve any singular layers and was implemented in order to examine the temporal and spatial stability of a three-dimensional compressible boundary-layer flow over a swept wing.

For the present work we attempted to adapt the methods used by BH but eventually concluded that we needed to use a more efficient algorithm here. The reasons for reaching this conclusion were twofold: first the form of the code relevant to the linearized problem (2.19) does not lend itself to easy modification for use in inhomogeneous problems such as (2.20). Second, and perhaps more importantly, BH conducted a small number of computations of solutions to (2.19) restricted to the three scaled frequency choices $\Omega_n = 1, 0, -1$. In order to execute the additional calculations required to compute the amplitude equation coefficients c_1 and c_2 as defined in (2.25) and to extend the results to a greater frequency range, it was felt that an improved algorithm was required.

We first outline our computational technique as far as it applies to solving the homogeneous system (2.19). This system can be characterized by the pair of equations

$$\frac{\mathrm{d}^4 V}{\mathrm{d}y^4}+\hat{\alpha}_v\frac{\mathrm{d}^2 V}{\mathrm{d}y^2}+\hat{\beta}_v\frac{\mathrm{d}V}{\mathrm{d}y}+\hat{\gamma}_v V+\hat{\delta}_v U=0, \quad \frac{\mathrm{d}^2 U}{\mathrm{d}y^2}+\hat{\alpha}_u U+\hat{\beta}_u V=0, \quad (3.1a, b)$$

where the coefficients $\hat{\alpha}_u, \hat{\alpha}_v, \ldots$ etc. are known functions of y. The system comprising (3.1) with associated boundary conditions typified by (2.19*c*) is an eigenvalue problem and was solved by considering (3.1) with only five of the homogeneous boundary conditions invoked. In addition, a normalization constraint was imposed so that (3.1) was solved subject to

$$U = V = 0, \quad \mathrm{d}U/\mathrm{d}y = 1 \quad \text{at} \quad y = 0, \tag{3.2a}$$

$$U = V = \mathrm{d}V/\mathrm{d}y \to 0 \quad \text{as} \quad y \to \infty. \tag{3.2b}$$

Iteration on the eigenvalue ensured that the sixth boundary condition $\mathrm{d}V/\mathrm{d}y = 0$ at $y = 0$ was satisfied. Specifically, in the context of problem (2.19), system (3.1), (3.2) was solved for complex-valued β_n for chosen frequency Ω_n, crossflow λ and vortex wavenumber k. Iteration on the imaginary part of β_n using a Newton iteration to vary λ enabled neutrally stable solutions to be found: cubic splines were used to track along the neutral curves.

As previously mentioned, a major benefit of the present algorithm over that used by BH is the much greater speed of calculation and this is due in part to the implementation of a variable mesh step. The equations (3.1) were discretized using central differencing on a grid running between $y = 0$ and $y = y^{(\infty)}$, where $y^{(\infty)}$ was chosen sufficiently large so that subsequent results were independent of its value. The

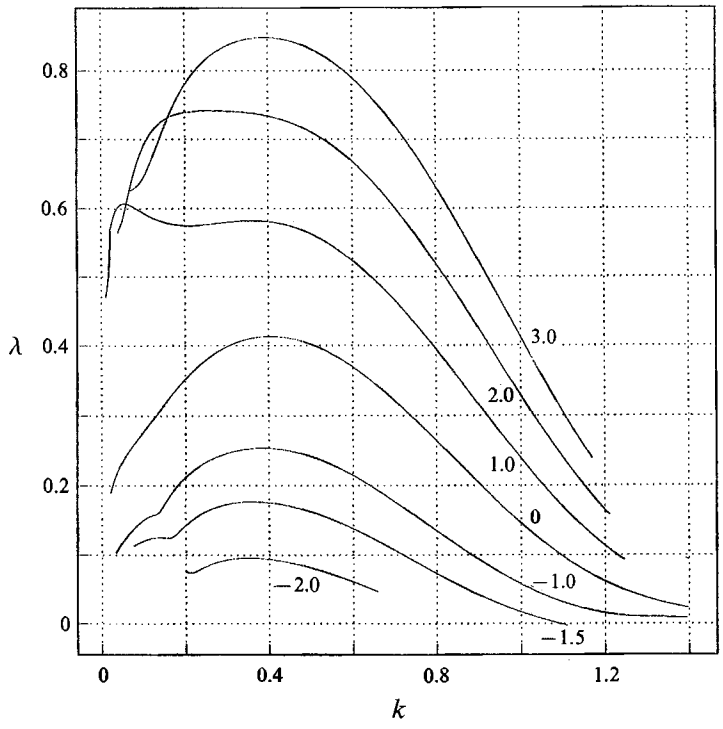

FIGURE 1. The crossflow parameter λ needed to ensure the neutral stability of vortices of various frequencies. $\Omega_n = 3.0, 2.0, 1.0, 0, -0.1, -1.5, -2.0$.

algorithm permits any grid discretization although for the current problem extensive testing revealed that it was adequate to limit the form of the grid to four distinct regions, in each of which the grid spacing was some constant with the closer spacing towards $y = 0$ and sparser grid points towards $y^{(\infty)}$. The choice of grid allowed us to use roughly one-third of the number of points needed by BH. Space limitations precludes more than this brief description of the numerical method, although a more detailed report of this aspect of this work may be obtained upon application to either author.

As a check on the method described above it was decided to repeat some of the linear calculations of BH to ensure consistency. Although BH did conduct a few computations relevant to non-neutral infinitesimal modes it should be remembered that our current concern is ultimately with describing the weakly nonlinear modes outlined in §2: disturbances which by definition are 'close' to the linear neutral stability curve. Therefore effort was concentrated on the neutral modes of BH. For frequencies $\Omega_n \in (-2, 3)$ figure 1 shows the crossflow parameter λ and figure 2 the parameter β_n as functions of the scaled vortex wavenumber k.

Certain trends surmized by BH on the basis of their numerical work restricted to three values of Ω_n are confirmed by our more extensive results. In particular it is seen that neutral modes appear to be possible over wide ranges of the wavenumber, and that for large k the crossflow needed to produce neutral modes is quite small (and is $\sim k^{-2}$ by the results of BH). Moreover, Denier *et al.* illustrated that for $\Omega_n = \lambda = 0$ all modes within the $O(G^{\frac{1}{5}})$-wavenumber regime are unstable; consequently crossflow is seen to have a stabilizing effect. A striking difference also occurs depending upon the sign of the scaled frequency Ω_n. For $\Omega_n \geqslant 0$ the neutral modes persist over the complete range

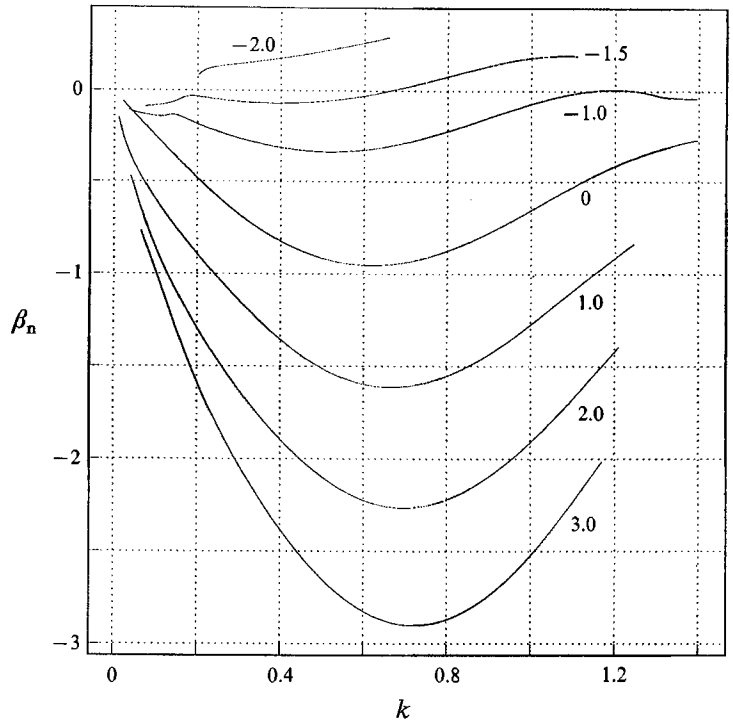

FIGURE 2. The streamwise variation parameter β_n of neutrally stable vortices of various frequencies. $\Omega_n = 3.0, 2.0, 1.0, 0, -1.0, -1.5, -2.0$.

of k, and as $k \to 0$ the crossflow λ required in order to preserve neutral modes tends to an $O(1)$ value. However, for $\Omega_n < 0$ BH and Bassom (1992) could not find such disturbances for all wavenumbers k and the neutral modes apparently disappeared for $k < k_c$, where k_c is some critical k. Figure 1 demonstrates that k_c increases as Ω_n becomes more negative.

For small wavenumbers k, figure 2 illustrates that the behaviour of the streamwise variation parameter β_n is also critically dependent upon Ω_n. For $\Omega_n \geqslant 0$, as $k \to 0$ then $\beta_n \to 0$ smoothly (and is proportional to $k^{\frac{1}{2}}$ by the results of BH). A contrasting situation occurs for $\Omega_n < 0$ for now both λ and β_n develop erratic behaviour as k decreases; behaviour which was also found in BH.

3.1. *The weakly nonlinear calculations*

Given the outline of the numerical method above, the implementation of the routines required to evaluate the amplitude equation coefficients c_1 and c_2 was straightforward. Once the homogeneous equations (2.19) were solved for the streamwise variation parameter β_n and scaled crossflow λ in terms of the given frequency Ω_n and wavenumber k and the respective eigenfunctions U_{11} and V_{11} deduced, it was a simple matter to evaluate the mean flow quantities U_{20} and Φ_0 defined in (2.21) and (2.22*c*). Next the solution of the inhomogeneous system (2.20) was required in order to determine the second-harmonic terms U_{22} and V_{22}. (The solution method for inhomogeneous problems had to be adapted from that used for homogeneous ones and details of the necessary modifications can be obtained from the authors.) After solving for the adjoint functions $\hat{F}(\psi)$ and $\hat{G}(\psi)$ as given by (2.23) the integrals z_1 and z_2 as defined in (2.24) were evaluated using Simpson's rule and the amplitude equation

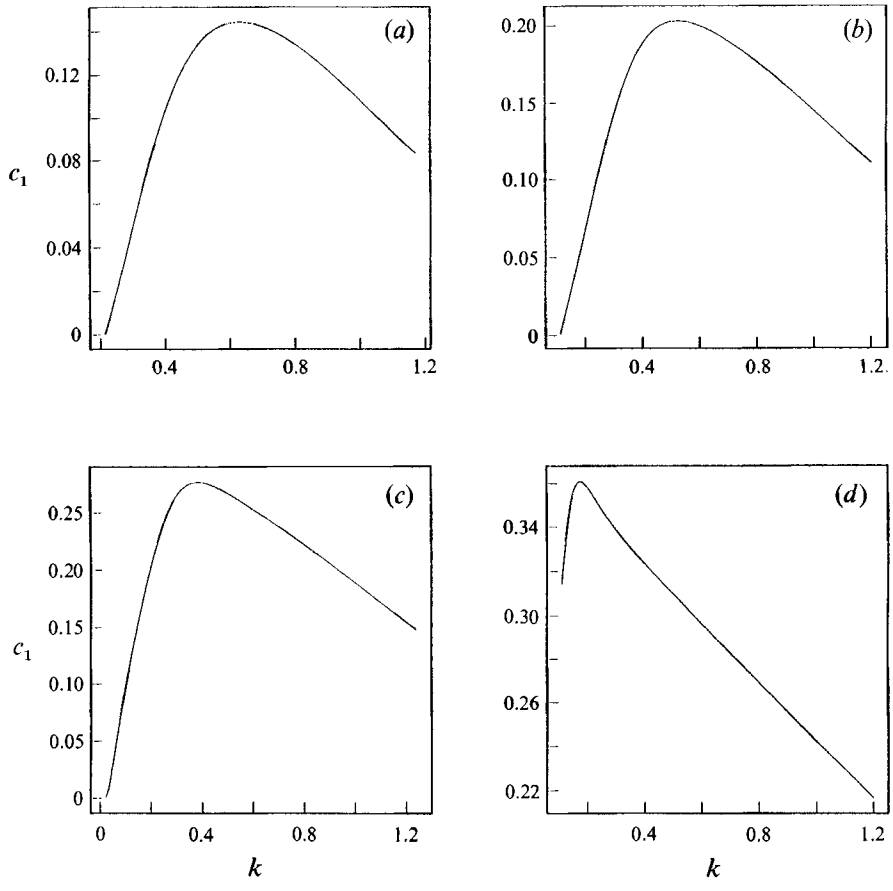

FIGURE 3(*a–d*). For caption see facing page.

coefficients c_1, c_2 thence deduced. The usual checks were made to ensure the accuracy of the numerical solutions of the systems (2.19), (2.20) and (2.23).

4. Remarks on the weakly nonlinear properties of the vortex modes

Implementation of the numerical procedures described in §3 led to the determination of the coefficients c_1 and c_2 appearing in the amplitude equation (2.25*b*). This equation demonstrates that the weak nonlinearity of the problem allows the existence of a threshold equilibrium amplitude A_e given by

$$|A_e|^2 = -c_1 \hat{\Omega}/c_2, \tag{4.1}$$

with $\hat{\omega} > 0$ or $\hat{\Omega} < 0$ as appropriate in order to ensure that the right-hand side of (4.1) is positive. Calculations were conducted for a variety of scaled frequencies Ω_n taking values between -2 and 3 and the results are summarized in figures 3–5. Figure 3 illustrates the dependence of the coefficient of the linear term in (2.25*b*) (i.e. c_1) upon Ω_n and the vortex wavenumber k. It is observed that $c_1 > 0$ across the whole range of wavenumber space, which indicates that according to linear theory a mode of frequency $\Omega_n + h^2\hat{\Omega}$ is unstable for $\hat{\Omega} > 0$ whereas it is stable for $\hat{\Omega} < 0$. This is to be expected as from figure 1 it may be deduced that for a fixed crossflow then as the frequency of the mode increases so it loses stability.

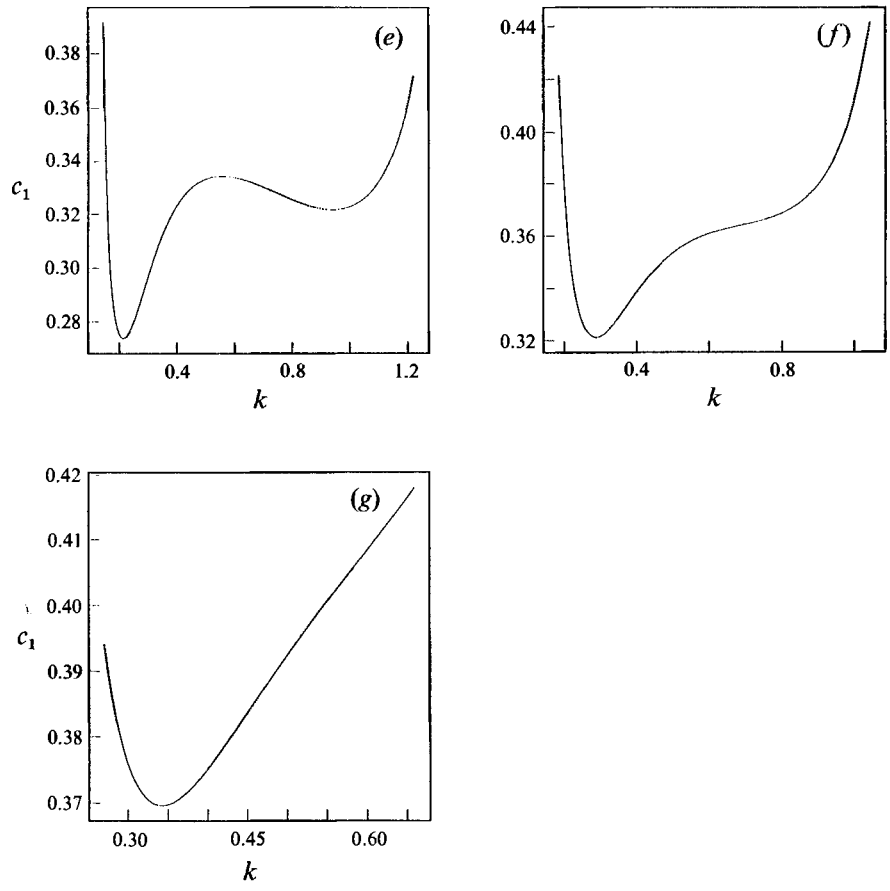

FIGURE 3. The coefficient c_1 of amplitude equation (2.25*b*) as a function of the vortex wavenumber k for (*a*) $\Omega_n = 3.0$, (*b*) 2.0, (*c*) 1.0, (*d*) 0, (*e*) -1.0, (*f*) -1.5 and (*g*) -2.0.

We turn now to interpret the findings summarized in figure 4 which illustrates the dependence of coefficient c_2 on k. This coefficient is of greater importance than c_1 for the sign of c_2 reveals the nature of the equilibrium amplitude A_e as defined in (4.1). For all Ω_n it is seen that $c_2 < 0$ and consequently the weak nonlinearity of the flow leads to a stabilization of the vortices. In this case vortices with initial amplitude less than A_e grow to A_e whereas those with initial size greater than A_e tend to diminish. However, it must be recalled that if the scaled amplitude A becomes too large the fundamental assumptions underlying weakly nonlinear theory are invalidated and a fully nonlinear account of the vortex structure is required.

Equation (4.1) trivially yields information concerning the equilibrium amplitude A_e, which is shown in figure 5 for the various values of Ω_n. Of course many features of this amplitude follow directly from the information portrayed in figures 3 and 4 and so require little additional comment. We mention first that for all the cases considered $c_2 < 0$ so that modes with perturbed frequency $\hat{\Omega} > 0$ would be expected to evolve to these equilibrium amplitudes whereas those with $\hat{\Omega} < 0$ would decay to zero. As $k \to \infty, |A_e| \to 0$ and as k decreases $|A_e|$ rises and reaches a maximum value and this maximum decreases with incresing $|\Omega_n|$. The form of figure 5(*a–c*) suggests that for vortices of scaled frequency $\Omega_n > 0$ those modes with low wavenumbers relative to the $O(G^{\frac{1}{5}})$ implied scaling would be more readily observed than those of greater

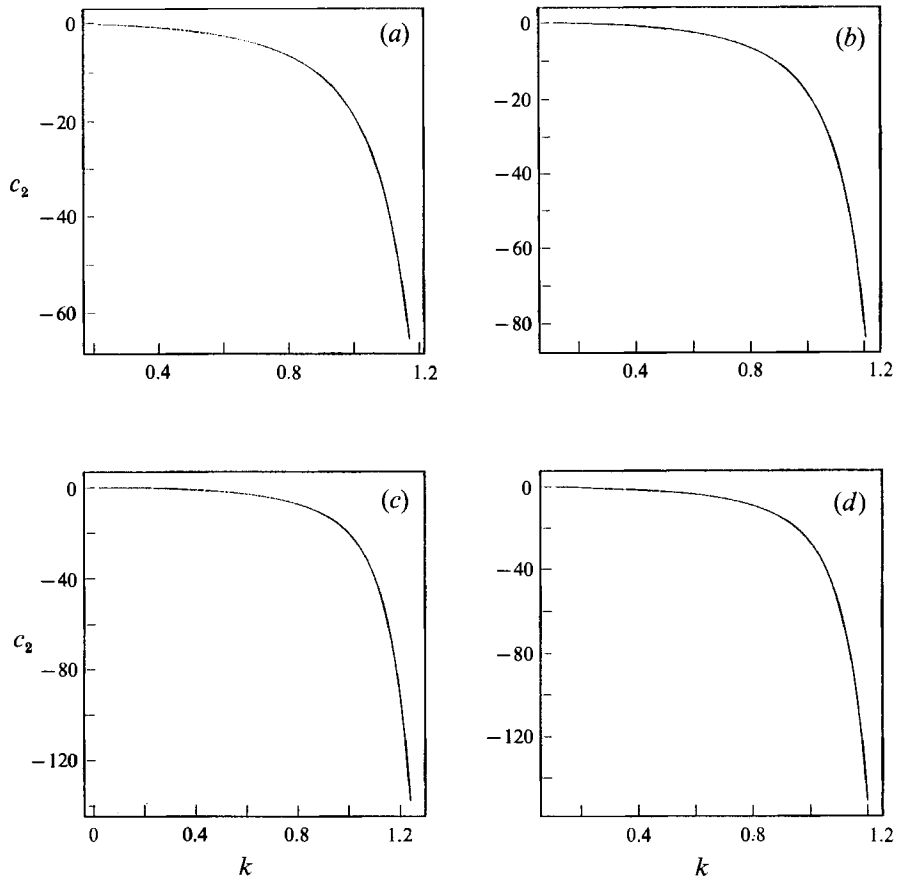

FIGURE 4(*a–d*). For caption see facing page.

wavenumber. It should also be noted that as $k \to 0$ the calculations became increasingly sensitive to the grid spacing used and the slight wobbles in the curves as $k \to 0$ are a direct consequence of this. In particular, the results for k less than about 0.1 are to be treated as being preliminary in nature. For Ω_n negative a number of the trends just described continue to persist. In particular, as Ω_n moves through increasingly more negative values $|A_e|$ decreases although its maximum value for any fixed frequency occurs at increasing values of k.

To conclude this description of the weakly nonlinear calculations it is worthwhile to briefly recall the more salient results. Importantly, whereas BH showed that the effect of crossflow is to stabilize the $O(G^{\frac{1}{5}})$-wavenumber modes according to a linearized theory, the above work has demonstrated that crossflow also stabilizes the modes on a weakly nonlinear basis. The corresponding equilibrium amplitudes calculated over a range of frequencies and wavenumbers reveals that the largest amplitudes are associated with near-stationary vortices and it can be tentatively proposed that these modes are the most likely candidates for practical observation. The analysis originally put forward by BH for small-wavenumber linearized vortices at scaled frequencies $\Omega_n > 0$ may be adapted to allow discussion of these modes using a weakly nonlinear approach and this is considered now.

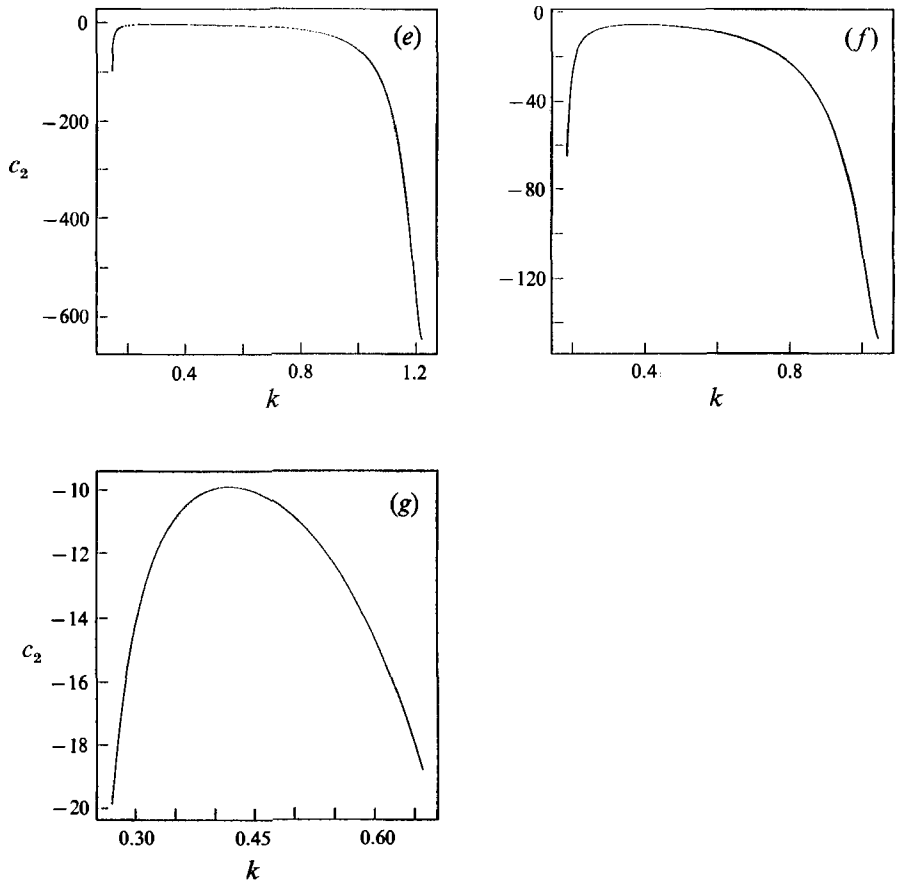

FIGURE 4. The coefficient c_2 of amplitude equation (2.25*b*) as a function of the vortex wavenumber k for (*a*) $\Omega_n = 3.0$, (*b*) 2.0, (*c*) 1.0, (*d*) 0, (*e*) −1.0, (*f*) −1.5 and (*g*) −2.0.

5. The low-wavenumber ($k \ll 1$) limit for $\Omega_n > 0$

The calculations presented in BH showed that when $\Omega_n > 0, k \ll 1$ the eigenfunctions U_{11} and V_{11} of system (2.19) are concentrated in a thin region near $\psi = 0$. They demonstrated that these functions assume a multi-zoned structure form and that the crossflow λ and streamwise variation parameter β_n required for neutral modes are given by

$$\lambda = \lambda_0 + \lambda_1 k^{\frac{1}{4}} + \ldots, \quad \beta_n = \beta_{n0} k^{\frac{1}{2}} + \beta_{n1} k^{\frac{3}{4}} + \ldots, \tag{5.1}$$

where all the constants are real valued. The asymptotic structure for the solution is summarized in figure 6 where it is shown that the configuration divides into a main zone, II, of thickness $O(k^{\frac{1}{2}})$ which contains a thin region I of depth $O(k^{\frac{3}{4}})$, supplemented by a viscous wall layer III of thickness $O(k)$, and a far-field zone, IV. It is to be recalled that the normalization chosen for all the numerical work in this paper is that $U'_{11} = 1$ at $\psi = 0$. Guided by this requirement it is easy to adopt the workings of BH to show that the most important contributions to the integrals defined in (2.24) occur within the zone I wherein it is convenient to write

$$\psi = k^{\frac{1}{2}}\psi_0 + k^{\frac{3}{4}}(\text{const} + \hat{\psi}). \tag{5.2a}$$

Here $\psi_0 \approx 1.47\Omega_n^{\frac{3}{8}}$ and the constant has a value which is of no importance for the

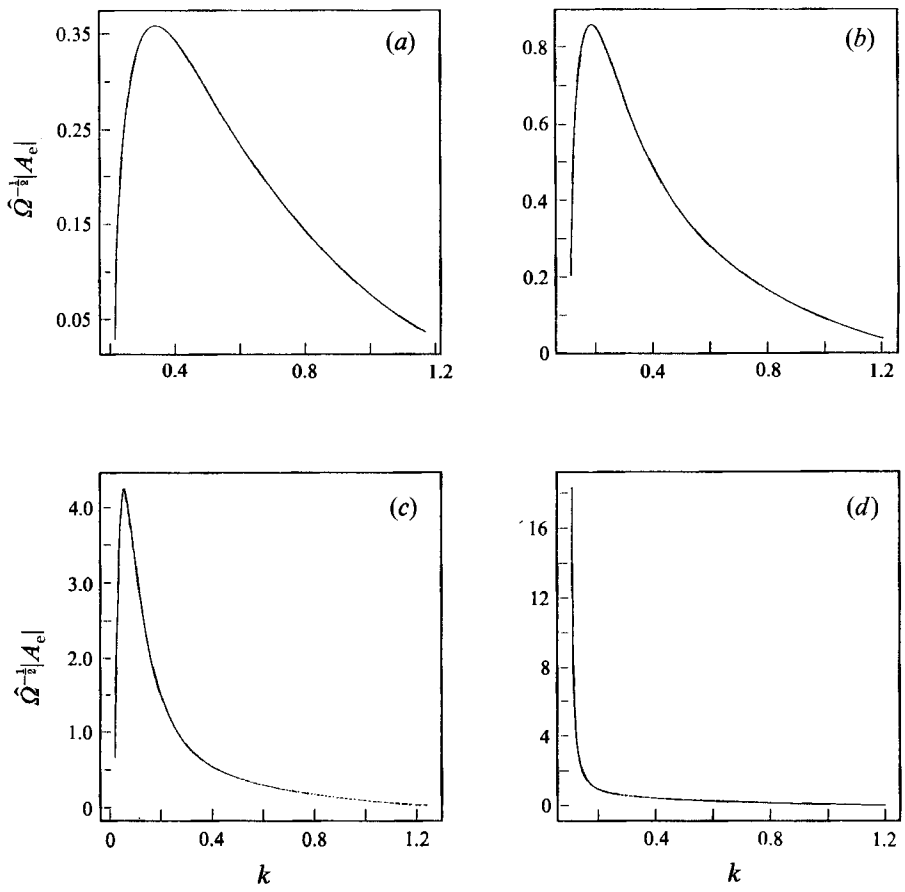

FIGURE 5(*a–d*). For caption see facing page.

current workings. Furthermore, in zone I the solutions U_{11} and V_{11} develop according to

$$U_{11} = k^{-\frac{1}{4}}\hat{U}_{11}(\hat{\psi}) + \ldots, \quad V_{11} = k^{\frac{1}{4}}\hat{V}_{11}(\hat{\psi}) + \ldots, \tag{5.2b}$$

where these functions satisfy

$$M_1(\hat{U}_{11}) = \hat{V}_{11}, \quad M_1(M_0\{\hat{V}_{11}\}) + 2\mathrm{i}\lambda_0\hat{V}_{11} = -\psi_0\hat{U}_{11}, \tag{5.2c, d}$$

and where we have made the definition $M_N(\Theta) \equiv \Theta'' - \mathrm{i}N(\hat{\Omega} + \lambda_0\hat{\psi}^2)\Theta$, in which the prime denotes differentiation with respect to $\hat{\psi}$. In (5.2*c*, *d*) $\hat{\Omega}$ is some constant and the solutions $\hat{U}_{11}$ and $\hat{V}_{11}$ are subject to the conditions

$$\hat{V}_{11} \to C/\hat{\psi}, \quad \hat{U}_{11} \to \mathrm{i}C/(\lambda_0\hat{\psi}^3) \quad \text{as} \quad |\hat{\psi}| \to \infty. \tag{5.2e}$$

The parameter C is chosen so that $U_{11}' = 1$ at $\psi = 0$ and elementary matching between the solutions valid in each of the regions sketched in figure 6 leads to

$$C \approx -0.21\mathrm{i}\Omega_{\mathrm{n}}^{\frac{7}{4}}. \tag{5.3}$$

The eigenproblem (5.2) was first solved by Hall (1985) who showed that $\psi_0\lambda_0^{-\frac{3}{2}} \approx 4.71$, $\hat{\Omega}\lambda_0^{-\frac{1}{2}} \approx -2.89$ (this latter value was misquoted in BH) which in turn gives $\lambda_0 \approx 0.46\Omega_{\mathrm{n}}^{\frac{1}{4}}$.

Following this work taken from BH it is straightforward to deduce the forms of the remaining functions within the thin zone I. The adjoint functions are

$$\hat{F} = \hat{\bar{F}}(\hat{\psi}) + \ldots, \quad \hat{G} = k\hat{\bar{G}}(\hat{\psi}) + \ldots,$$

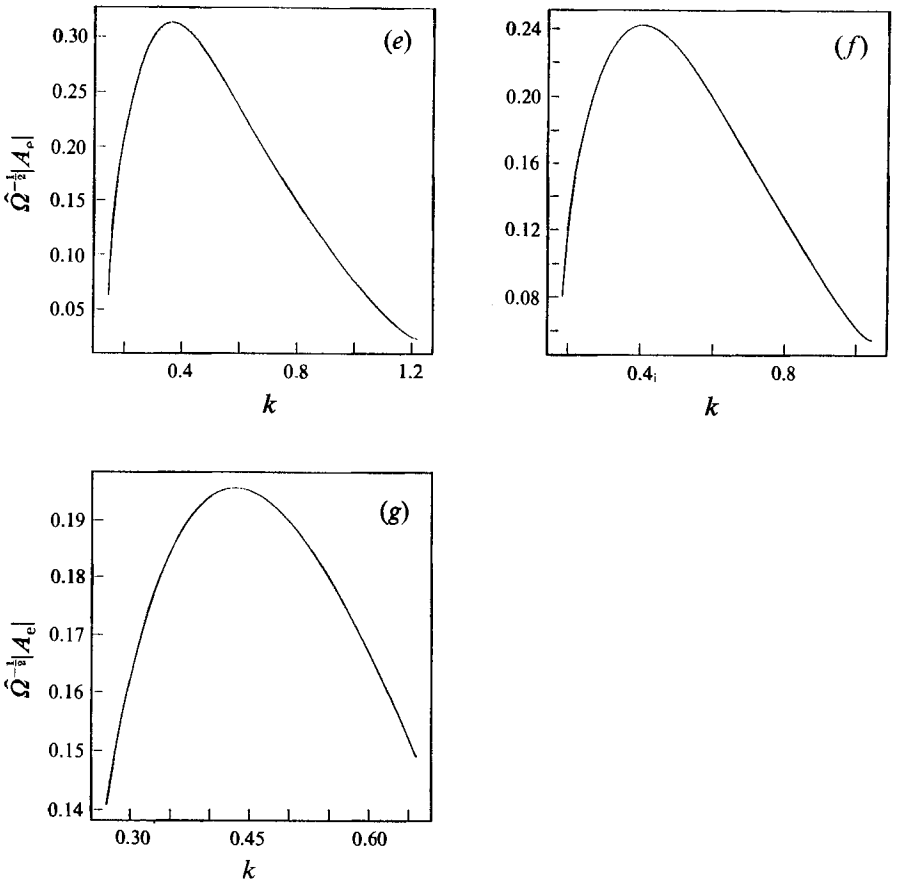

FIGURE 5. The equilibrium amplitude $\hat{\Omega}^{-\frac{1}{2}}|A_e|$ (defined by (4.1)) as a function of the vortex wavenumber k for (*a*) $\Omega_n = 3.0$, (*b*) 2.0, (*c*) 1.0, (*d*) 0, (*e*) -1.0, (*f*) -1.5 and (*g*) -2.0.

where $$M_1(\hat{\bar{F}}) + \psi_0 \hat{\bar{G}} = 0, \quad M_1(M_0(\hat{\bar{G}})) - 4i\lambda_0 \hat{\bar{\psi}}(d\hat{\bar{G}}/d\hat{\bar{\psi}}) = \hat{\bar{F}}, \tag{5.4a, b}$$

subject to the conditions that $\hat{\bar{F}} \propto \hat{\bar{\psi}}^{-5}$ and $\hat{\bar{G}} \propto \hat{\bar{\psi}}^{-3}$ as $|\hat{\bar{\psi}}| \to \infty$. Furthermore, $U_{22} = k^{-\frac{1}{4}}\hat{U}_{22} + \ldots$, $V_{22} = k^{\frac{1}{4}}\hat{V}_{22} + \ldots$, where $\hat{U}_{22}$ and $\hat{V}_{22}$ are odd-valued functions satisfying

$$M_2(\hat{U}_{22}) - \hat{V}_{22} = \hat{U}'_{11}\hat{V}_{11} - \hat{U}_{11}\hat{V}'_{11}, \tag{5.5a}$$

$$M_2(M_0(\hat{V}_{22})) + 4i\lambda_0 \hat{V}_{22} + 4\psi_0 \hat{U}_{22} = 2(\hat{V}_{11}\hat{V}'''_{11} - 2\hat{V}'_{11}\hat{V}''_{11}), \tag{5.5b}$$

subject to the constraints that $\hat{U}_{22} = O(\hat{\bar{\psi}}^{-7})$ and $\hat{V}_{22} = O(\hat{\bar{\psi}}^{-5})$ as $|\hat{\bar{\psi}}| \to \infty$. Finally, within zone I the functions U_{20} and Φ_0 are

$$U_{20} = k^{-\frac{1}{4}}\hat{U}_{20}(\hat{\bar{\psi}}) + \ldots, \quad \Phi_0 = k^{\frac{1}{4}}\hat{\Phi}_0(\hat{\bar{\psi}}) + \ldots,$$

where $$\hat{U}_{20} = \int_{-\infty}^{\hat{\bar{\psi}}} (\hat{U}_{11}\hat{V}^*_{11} + \hat{U}^*_{11}\hat{V}_{11})\, d\hat{\bar{\psi}}, \quad \hat{\Phi}_0 = \int_{-\infty}^{\hat{\bar{\psi}}} \left(\hat{V}_{11}\frac{d\hat{V}^*_{11}}{d\hat{\bar{\psi}}} - \hat{V}^*_{11}\frac{d\hat{V}_{11}}{d\hat{\bar{\psi}}}\right) d\hat{\bar{\psi}}. \tag{5.6}$$

Formally, it is possible to use the expansions given above to deduce the forms of the various flow quantities in each of the remaining regions II–IV. However, tedious but straightforward manipulations verify that the dominant contributions to the expressions (2.24*a–c*) arise from within zone I.

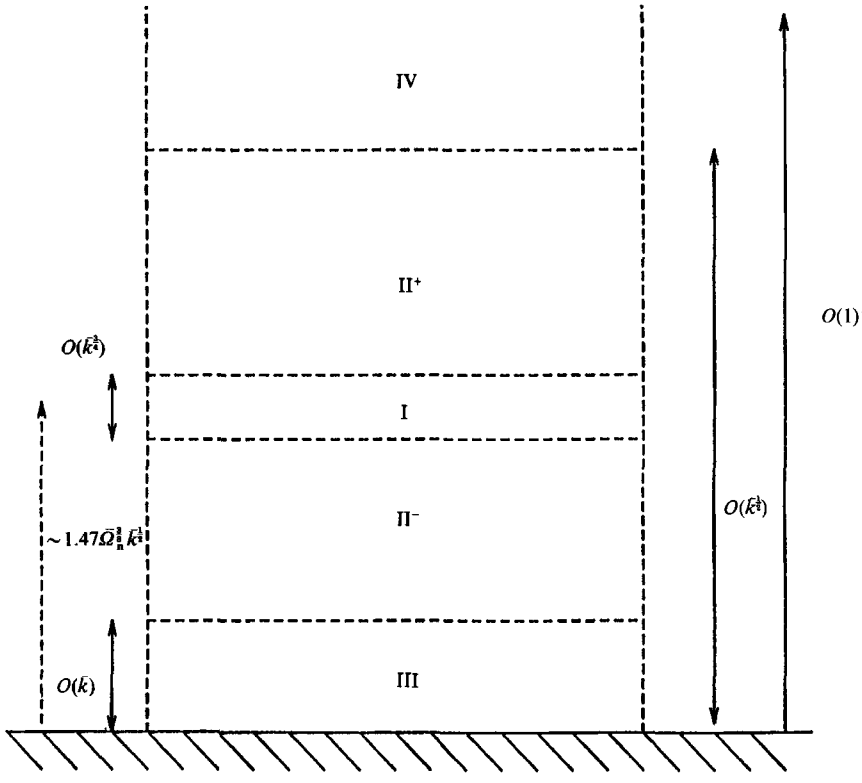

FIGURE 6. Schematic diagram of the asymptotic structure of the solution of homogeneous system (2.19) for the case of small vortex wavenumber $k \ll 1$. The solution configuration divides into four distinct zones: Zone I is a thin region of depth $O(k^{\frac{3}{4}})$ at a distance $\sim 1.47\Omega_{\mathrm{n}}^{\frac{3}{8}} k^{\frac{1}{8}}$ from the wall. This zone is embedded within II, a region of thickness $O(k^{\frac{1}{4}})$. The structure has an additional viscous layer at the wall, zone III, which enables the boundary conditions there to be met. Finally, a region IV of depth $O(1)$ facilitates the exponential decay of the disturbance solutions far from the wall.

The systems (5.2), (5.4) and (5.5) were solved using adaptations of our general technique and the amplitude equation coefficients were found to take the forms

$$c_1 \approx 0.2\Omega_{\mathrm{n}}^{-\frac{3}{8}} k^{\frac{1}{4}} + \ldots, \quad c_2 \approx -7\Omega_{\mathrm{n}}^{\frac{11}{8}} k^3 + \ldots, \tag{5.7a, b}$$

as $k \to 0$. These asymptotic predictions provided reasonable agreement with the numerical results discussed in the preceding section. Results (5.7) then imply that the equilibrium amplitude

$$|A_{\mathrm{e}}| \approx 0.2\Omega_{\mathrm{n}}^{-\frac{7}{8}} k^{-\frac{11}{8}} \Omega^{\frac{1}{2}},$$

which again suggests that it is the low-wavenumber and relatively low-frequency modes that have the greatest equilibrium amplitudes. However there is evidence from figure 5(*a–c*) that as k decreases, the accuracy of our computational work deteriorates. One difficulty with the prediction of A_{e} as $k \to 0$ is provided by the extreme smallness of the coefficient c_2 (see (5.7*b*)). Clearly, tiny inaccuracies in the evaluation of c_2 can have drastic consequences for the resulting value of $|A_{\mathrm{e}}|$. As $k \to 0$ it has been demonstrated that the entire solution structure becomes compressed against the wall and then the numerical resolution of the distinct zones sketched in figure 6 is rendered increasingly difficult. As mentioned previously, we estimate that for wavenumbers k less than about 0.1 our solutions can only be regarded as tentative at best.

The scalings described above fail as $\Omega_n \to 0$ for in this limit the thin layer I moves towards the wall and BH demonstrated that when $\Omega_n = O(k^{\frac{4}{7}})$ this layer merges with the viscous wall layer III. Within the wall layer the governing equations now take the forms

$$\left(\frac{d^2}{d\tilde{\xi}^2} - i\tilde{\Omega} - i\tilde{\beta}\tilde{\xi} - i\tilde{\lambda}\tilde{\xi}^2\right)\tilde{U} = \tilde{V}, \quad \left(\frac{d^2}{d\tilde{\xi}^2} - i\tilde{\Omega} - i\tilde{\beta}\tilde{\xi} - i\tilde{\lambda}\tilde{\xi}^2\right)\frac{d^2\tilde{V}}{d\tilde{\xi}^2} + 2i\tilde{\lambda}\tilde{V} = -\tilde{\xi}\tilde{U}, \quad (5.8a, b)$$

where the tilde denotes quantities scaled on suitable powers of k (fuller details are given in BH and Bassom 1992). In particular, $\Omega_n = k^{\frac{4}{7}}\tilde{\Omega}$ and these wall-layer equations need to be solved subject to the conditions

$$\tilde{U}, \quad \tilde{V} \quad \text{and} \quad d\tilde{V}/d\tilde{\xi} \to 0 \quad \text{at} \quad \tilde{\xi} = 0 \quad \text{and as} \quad \tilde{\xi} \to \infty. \qquad (5.8c)$$

Bassom (1992) used the numerical code of Malik *et al.* (1982) to solve (5.8) for a selection of values of $\tilde{\Omega}$. As $\tilde{\Omega} \to \infty$ he showed how these low-frequency modes match with those for which $\Omega_n = O(1)$ but he could only manage to obtain solutions of (5.8) for $\tilde{\Omega}$ greater than $\tilde{\Omega}_c \approx -3.3$. The work of Bassom (1992) was prompted in part by the finding of BH concerning the low-wavenumber structure outlined by (5.2) above. The asymptotic regions found by BH are only valid for positive values of Ω_n and that paper made tentative suggestions concerning possible configurations when $\Omega_n < 0$. In particular, a critical-layer-type problem was proposed but no attempt was made to solve this. Subsequent calculations failed to find a solution and Bassom (1992) hoped to connect the $\Omega_n > 0$ and $\Omega_n < 0$ cases by investigating the intermediate problem where $\Omega_0 = k^{\frac{4}{7}}\tilde{\Omega}$ by examining the numerical solutions of (5.8) as $\tilde{\Omega} \to -\infty$. However, the existence of the cutoff frequency $\tilde{\Omega}_c$ below which numerical solutions were unattainable thwarted this aim.

The system (5.8) was re-solved using the method developed in the current work. As in Bassom (1992), difficulties were encountered as $\tilde{\Omega}_c$ was approached. Closer studies of this phenomenon revealed that as $\tilde{\Omega} \to \tilde{\Omega}_c$ the eigensolution migrates from the wall $\tilde{\xi} = 0$ and thus becomes almost completely independent of the boundary conditions imposed at the wall. Therefore the solution becomes insensitive to the values of the eigenparameters and numerical convergence is impossible to obtain. This type of behaviour typically occurs whenever a 'null space' of the system is approached and indicates that the elimination techniques employed to solve the discretized equations need to be replaced by a scheme which directly inverts the entire discretized set (such schemes are termed 'global methods'). This is computationally extremely expensive but it does lead to a determination of a spectrum of eigenvalues of the problem.

This difficulty, which arises when a null space of a problem is encountered, also provides the explanation for some of the other deficiencies in our numerical work to date. In figures 1 and 2 where neutral curves were presented it is noted that as Ω_n becomes progressively more negative the wavenumber range over which results were obtained diminishes. Investigations have shown that this is again due to approaching a null space of the appropriate system (2.19). BH also made some remarks concerning the properties of high-wavenumber modes. They formulated an eigenproblem appropriate to these vortices but did not solve this. It was noted that their calculations of solutions of the homogeneous system (2.19) failed for values of k larger than about 1.4 and our further researches have confirmed that the reason for this failure is that the null space of system (2.19) is approached at about this value of k.

In order to develop our findings of this paper further work is needed to investigate the global numerical methods. Preliminary runs with a small number of grid points

have been conducted for the eigenproblem (5.2) and for the small-frequency problem (5.8). Results for this latter problem have revealed the existence of solutions for $\tilde{\Omega}$ less than the cutoff value $\tilde{\Omega}_c$. This indeed suggests that the previous problems for $\tilde{\Omega} < \tilde{\Omega}_c$ are entirely numerically based and have no physical significance. As yet there are too few results from the computationally intensive global method to justify a fuller discussion here. However, it is probable that developments with these ideas will lead to an improved explanation of the large-wavenumber and the small-k, $\Omega_n < 0$ limits.

6. Discussion

The main conclusion of our work has been that over all the wavenumbers and frequencies investigated the influence of weak nonlinearity is stabilizing and the consequent supercritical equilibrium amplitudes have been evaluated. These amplitudes tend to be largest for vortices of small wavenumber and frequency relative to the initial scalings and suggest that it is these modes that would appear to be the most likely to be observed in practice. A limited asymptotic study has been accomplished which yields indications of the solution characteristics for small k and positive scaled frequencies Ω_n. However, the corresponding work for negative Ω_n and that relevant to large wavenumbers k was not completed owing to difficulties in encountering null spaces of the governing differential systems. As reported in the previous section, preliminary work has begun using more appropriate numerical methods in order to circumvent these problems. We feel that these calculations are important for the following reason. The work described by BH and that here has conclusively demonstrated that both the linear and weakly nonlinear properties of these viscous vortices are critically dependent upon the sign of the scaled frequency and crossflow λ. For any particular boundary layer either case may be the more relevant (depending upon the signs of the scaling quantities within (2.15)) and so it is desirable that both eventualities are analysed properly. Whereas the solution properties are now reasonably well understood for $\Omega_n > 0$ this understanding is clearly deficient for $\Omega_n < 0$ and work on this latter case is continuing.

One advantage of concentrating on the $O(G^{\frac{1}{5}})$-wavenumber modes, apart from the fact that these are the most unstable linear vortices for a two-dimensional boundary layer, is that the structure of the disturbance permits all the basic flow quantities that are functions of the particular boundary layer to be scaled out of the problem leaving a system of equations which is valid for a wide variety of three-dimensional flows. Consequently the scalings (2.15) would need to be reversed in order to assess the implications of our findings for any specified flow.

We emphasize that the validity of the study here is restricted to the wavenumber regime $k = O(G^{\frac{1}{5}})$. As the scaled wavenumber k_0 defined by (2.5b) tends to zero the vortices become inviscid in character and the Stuart–Watson approach becomes invalidated. The theory is then replaced by a revised structure which is, to the best of our knowledge, as yet unknown. For $k_0 \to \infty$ a match is obtained with the work of Hall (1985). This paper showed, using linear theory, that neutral Görtler vortices were possible at crossflows smaller than those encountered in this paper. Such vortices are likely to be governed by an adaptation of the 'mean-field' theory valid in the vicinity of the right-hand branch of the usual neutral curve appropriate to vortices in a two-dimensional boundary layer. We have not attempted to obtain the match between our weakly nonlinear account and this mean-field adaptation as such a structure would come into play at crossflow values smaller than those considered here, at which stage all the $O(G^{\frac{1}{5}})$-wavenumber modes would still be linearly unstable.

A question that merits attention is that pertaining to the nature of the fully nonlinear properties of viscous vortices in three-dimensional boundary layers. The investigation of Denier & Hall (1993) described in the introduction has concentrated upon the two-dimensional version of this problem and showed that in general the vortex suffers a finite-distance algebraic breakdown as it develops downstream. Denier & Hall were unable to conduct a weakly nonlinear analysis of the type discussed here for in the two-dimensional boundary layer there are no neutral modes of wavenumber $O(G^{\frac{1}{5}})$. The results of BH and the extensions presented in the current work show that the effect of three-dimensionality is to stabilize the vortex mode. Therefore the three-dimensional version of Denier & Hall (1993) would be most valuable in deciding whether fully nonlinear or crossflow effects are the more important. The former induces a catastrophic breakdown in the flow whereas the latter effect is stabilizing and so it can be anticipated that there may well be a delicate balance between the two.

BH investigated the linear stability properties of both $O(1)$-wavenumber inviscid modes and the $O(G^{\frac{1}{5}})$-wavenumber vortices considered in this paper. They attempted to resolve the question as to which mode is the more likely candidate for practical observation. By carrying out a linearized receptivity calculation of the type given in Denier *et al.* (1991) relevant to Görtler vortices in two-dimensional boundary layers, BH were able to show that wall roughness is a more efficient stimulator of the viscous modes than the inviscid ones and thus the viscous modes might be the easier to generate experimentally. However, they also pointed out that as the crossflow increases, the growth rates of the inviscid modes increase to become larger than the viscous rates. Thus beyond a certain crossflow size the observed instability may well be of Rayleigh-type character.

In many practical situations where Görtler vortices are thought to be a likely cause for transition the basic state is three-dimensional. Our work has demonstrated that a crossflow of small size $O(Re^{-\frac{1}{2}}G^{\frac{2}{5}})$ is suffucient to stabilize vortex modes according to a weakly nonlinear basis, but the results of Denier & Hall (1993) indicate that full nonlinearity of the disturbance may well lead to rapid breakdown. The relative importance of these crossflow and nonlinear mechanisms is a matter of some interest, which can only be resolved by extending our findings to the fully nonlinear regime. This problem should obviously be a topic of careful theoretical and practical investigations of the Görtler mechanism in three-dimensional boundary layers.

The authors wish to thank Dr Craig Streett of NASA Langley for guidance regarding the nature of null spaces of differential systems. The research of S. R. O. was supported by the National Aeronautics and Space Administration under NASA contract No. NAS1-18605 while he was in residence at the Institute for Computer Applications in Science and Engineering (ICASE), NASA Langley Research Center, Hampton, VA 23665, USA. A. P. B. would like to thank ICASE for their support and hospitality during a visit whilst part of this work was carried out.

We are both grateful to all three referees and the editor for their numerous constructive and helpful comments on this work.

REFERENCES

BASKARAN, V. & BRADSHAW, P. 1988 Decay of spanwise inhomogeneities in a three-dimensional turbulent boundary layer over an infinite swept concave wall. *Exps Fluids* **6**, 487–492.

BASSOM, A. P. 1992 Time dependent inviscid vortices in three-dimensional boundary layers. *Q. J. Mech. Appl. Maths* **45**, 339–362.

BASSOM, A. P. & HALL, P. 1991 Vortex instabilities in three-dimensional boundary layers: the relationship between Görtler and crossflow vortices. *J. Fluid Mech.* **232**, 647–480 (referred to herein as BH).

DENIER, J. P. & HALL, P. 1993 On the nonlinear development of the most unstable Görtler vortex mode. *J. Fluid Mech.* **247**, 1–16.

DENIER, J. P., HALL, P. & SEDDOUGUI, S. 1991 On the receptivity problem for Görtler vortices: vortex motion induced by wall roughness. *Phil. Trans. R. Soc. Lond.* A **335**, 51–85.

GREGORY, N., STUART, J. T. & WALKER, W. S. 1955 On the stability of three dimensional boundary layers with application to the flow due to a rotating disk. *Phil. Trans. R. Soc. Lond.* A **248**, 155–199.

HALL, P. 1982*a* Taylor–Görtler vortices in fully developed or boundary layer flows. *J. Fluid Mech.* **124**, 475–494.

HALL, P. 1982*b* On the nonlinear evolution of Görtler vortices in non-parallel boundary layers. *J. Inst. Maths Applics* **29**, 173–196.

HALL, P. 1983 The linear development of Görtler vortices in growing boundary layers. *J. Fluid Mech.* **130**, 41–58.

HALL, P. 1985 The Görtler vortex instability mechanism in three-dimensional boundary layers. *Proc. R. Soc. Lond.* A **399**, 135–152.

HALL, P. 1988 The nonlinear development of Görtler vortices in growing boundary layers. *J. Fluid Mech.* **193**, 247–266.

HALL, P. 1990 Görtler vortices in growing boundary layers: the leading edge receptivity problem, linear growth and the nonlinear breakdown stage. *Mathematika* **37**, 151–189.

MALIK, M. R., CHUANG, S. & HUSSAINI, M. Y. 1982 Accurate numerical solution of the compressible linear stability equations. *Z. Angew. Math. Phys.* **33**, 189–201.

STUART, J. T. 1960 On the nonlinear mechanics of wave disturbances in stable and unstable parallel flows. Part 1. The basic behaviour in plane Poiseuille flow. *J. Fluid Mech.* **9**, 353–370.

TIMOSHIN, S. N. 1990 Asymptotic analysis of a spatially unstable Görtler vortex spectrum. *Fluid Dyn.* **25**, 25–33.

WATSON, J. 1960 On the nonlinear mechanics of wave disturbances in stable and unstable parallel flows. Part 2. The development of a solution for plane Poiseuille and plane Couette flow. *J. Fluid Mech.* **9**, 371–389.